LA-UR-04-1826

Title:	*Modeling Thermal-Hydrologic-Chemical (THC) Coupled Processes with Application to Underground Nuclear Tests at the Nevada Test Site: A "Grand Challenge" Supercomputing Problem*
Author(s):	Peter C. Lichtner (lichtner@lanl.gov) Andrew Wolfsberg
Submitted to:	MOU Workshop: *Conceptual Model Development for Subsurface Reactive Transport Modeling of Inorganic Contaminants, Radionuclides, and Nutrients*
Location:	La Posada Hotel, Albuquerque, NM
Time:	April 20 – 22, 2004
Date Prepared:	March 29, 2004

TABLE OF CONTENTS

Modeling Thermal-Hydrologic-Chemical (THC) Coupled Processes with Application to Underground Nuclear Tests at the Nevada Test Site: A "Grand Challenge" Supercomputing Problem

P.C. Lichtner and A.V. Wolfsberg
Los Alamos National Laboratory, Los Alamos, New Mexico
lichtner@lanl.gov

1 INTRODUCTION

At the Nevada Test Site (NTS), the continental nuclear weapons testing site in the United States, 828 underground tests were conducted between 1951 and 1992 (DOE, 2000). This study is focused on the BENHAM underground nuclear test conducted on December 19, 1968. During the period from 1996 to 1998, a number of radionuclides consisting of ^{3}H, ^{137}Cs, ^{60}Co, ^{152,154,155}Eu, ^{237}Np, ^{239,240}Pu, ^{241}Am, ^{14}C, ^{36}Cl, ^{99}Tc, ^{129}I, ^{90}Sr, and ^{214}Pb were detected in trace quantities 1.3 km from the BENHAM test. The radionuclides were discovered in well ER-20-5 #3, sampling a lava formation located near the depth of the working point (WP), and well ER-20-5 #1, sampling the TSA welded tuff aquifer located some 500 m above the WP situated at a depth of 1402 m (Wolfsberg et al., 2002; Kersting et al., 1999). Kersting et al. (1999) report that isotopic fingerprinting indicated the ^{239,240}Pu originated at BENHAM, rather than the closer TYBO test executed on May 14, 1975, at a depth of 765 m, and that in both aquifers ^{239,240}Pu was associated with colloids. These observations indicate an approximate travel time for ^{239,240}Pu on the order of 30 years or shorter. The BENHAM test, with an announced official yield of 1.15 megatons (DOE, 2000), produced a spherical cavity estimated at 200 m in diameter. The bottom of the cavity filled with melted rock, referred to as melt glass. A cylindrical, rubblized, chimney formed as rock above the cavity collapsed, extending from the working point of the test to above the TSA welded tuff aquifer. The melt glass is thought to contain a large proportion of the radionuclide inventory for Pu, whereas other less refractory radionuclides are distributed between the melt glass and the surrounding chimney material (Pawloski et al., 2001). A puzzling question arises as to how ^{239,240}Pu (and other radionuclides) could have migrated from the BENHAM test to two distant wells located in aquifers that apparently do not interact with one another, except through the chimney system created by the test. In addition, the radionuclides in question have wide ranging chemical properties including sorptive, solubility, and complexing affinity. This contribution attempts to elucidate the mechanisms responsible for transporting this diverse group of radionuclides over the relatively short times and long distances observed at the NTS.

Because the geometry of the system is intrinsically 3-D, consisting of a vertical cylindrical chimney with melt glass at the bottom embedded in a horizontally layered medium with an ambient lateral flow gradient, simulations to be at all realistic must be carried out in three spatial dimensions. In addition, field length scales for the system range from 100 m corresponding to the chimney radius to 1.3 km equal to the distance from the BENHAM test WP to the observation wells. Within the cavity-chimney-melt-glass region it is necessary to resolve length scales on the order of 10 m or less to capture thermal effects resulting in highly tortuous convection cells. These considerations necessitate the use of high performance computing for all but the coarsest grids.

To explain the observed radionuclide breakthrough behavior, a complex thermal, hydrologic, and chemical (THC) coupled process model is called for. However, before embarking on this endeavor with its extensive data requirements, it is prudent to take a more simplified approach to first explore the complex interplay between heat, fluid flow, and solute transport resulting from an underground test. To this end, the focus here is on coupling heat and fluid flow processes while using a relatively simple formulation of non-reactive solute transport and calibrating the predicted breakthrough times to well data. Reserved for future studies is the additional coupling of more complex chemical processes. Nevertheless, interpretation of results obtained

from the simplified model provides unique insights and raises interesting questions into system responses to a transient heat source and migration of reactive and non-reactive solutes in fractured rock aquifers.

2 RADIONUCLIDE MIGRATION FROM AN UNDERGROUND NUCLEAR TEST AT THE NEVADA TEST SITE

2.1 Conceptual Model

The conceptual model used to describe radionuclide migration from an underground nuclear test consists of a near-field region composed of the chimney-cavity-melt-glass system, and a far-field region consisting of the surrounding host rock (Pawloski et al., 2001; Wolfsberg et al., 2002). Following the detonation and rewetting of the near-field region, vigorous convection takes place in the high permeability chimney as buoyant flow driven by heat released from the melt glass moves up the chimney carrying radionucldes to the overlying aquifers. The host rock is modeled as a layered medium with effective homogeneous properties for each stratigraphic unit. The rubbleized chimney is modeled as a porous medium with relatively high permeability and high porosity. In a highly simplified description of this system, three conservation equations are needed to describe these processes: mass, energy, and solute corresponding to Eqns. (1a), (1b), and (1c). A single continuum description is employed based on effective properties for porosity, permeability, and other material quantities to represent flow and transport through a fractured porous medium [see c.f. Lichtner (2000)]. In a fractured porous medium, in the limit when full equilibration occurs between fracture and matrix continua due to small fracture spacing or slow flow rate, the equivalent continuum representation of the fractured medium is approached. For an upscaled, equivalent continuum formulation, effective porosity and permeability are related to intrinsic fracture, matrix properties (subscripts f, m), by the expressions $\phi = \epsilon_f \phi_f + (1-\epsilon_f)\phi_m$ and $k = \epsilon_f k_f + (1-\epsilon_f)k_m$, where ϵ_f refers to the fracture volume fraction. In this case, fracture and matrix porewater concentrations are equal. However, for the system under consideration it is not expected that these conditions apply due to the high flow rate and large fracture spacing. This hypothesis is tested and discussed below. Although in general, radioactive decay, retardation, and colloid velocity enhancement factors are needed to describe solute transport, in what follows a single non-reactive tracer is considered ($R = 1$). Transport of sorbing radionuclides is presumed to occur via colloids. For colloids to be effective, it would also seem necessary that sorption on colloids be irreversible, thereby minimizing competition with host rock minerals. In the presence of reversible sorption, colloids must compete with stationary minerals requiring a large colloid concentration to achieve a comparable cation exchange capacity or surface site density (Honeyman and Ranville, 2002). Presumably two pools of the sorbing radionuclides ^{137}Cs and ^{239,240}Pu are present, a highly mobile fraction that becomes irreversibly attached to colloids, and a immobile fraction that remains held to mineral surfaces within the chimney and possibly along the flow path outside the chimney. Because we are primarily interested in describing breakthrough at the ER-20-5 wells, we need only be concerned with the mobile radionuclide fraction. This fraction is presumed to consist of nonsorbable species (such as ^{3}H and ^{36}Cl), in addition to sorbable species (such as ^{137}Cs and ^{239,240}Pu). These latter species are assumed to be irreversibly sorbed

THC Coupled Processes:

$$\frac{\partial}{\partial t}\phi\rho + \boldsymbol{\nabla}\cdot\boldsymbol{F}_\rho = 0 \qquad (1a)$$

$$\frac{\partial}{\partial t}\left[\phi\rho U + (1-\phi)\rho_r c_r T\right] + \boldsymbol{\nabla}\cdot\boldsymbol{F}_e = 0 \qquad (1b)$$

$$\frac{\partial}{\partial t}\phi RC + \boldsymbol{\nabla}\cdot\boldsymbol{F}_C + \lambda C = 0 \qquad (1c)$$

Flux:

$$\boldsymbol{F}_\rho = \boldsymbol{q}\rho \qquad (2a)$$

$$\boldsymbol{F}_e = \boldsymbol{q}\rho H - \kappa\boldsymbol{\nabla}T \qquad (2b)$$

$$\boldsymbol{F}_C = f_c\boldsymbol{q}C - \phi D\boldsymbol{\nabla}C \qquad (2c)$$

Darcy Velocity:

$$\boldsymbol{q} = -\frac{k}{\mu}\left(\boldsymbol{\nabla}p - \rho g\hat{\boldsymbol{z}}\right) \qquad (2d)$$

Symbols: temperature T, pressure p, solute concentration C, porosity ϕ, density ρ, energy U, enthalpy H, permeability k, viscosity μ, acceleration of gravity g, rock heat capacity c, thermal conductivity κ, rock density ρ_r, retardation R, collide enhancement factor f_c, dispersion/diffusion coefficient D, decay constant λ.

onto colloids and to undergo colloid-facilitated transport with little or no retardation. Thus in either case, it can be assumed that radionuclide migration is described by the non-reactive solute transport equation.

2.2 Model Implementation

The computational domain used in the simulations measures 1.5 km $\times$ 500 m $\times$ 1050 m, encompassing both the BENHAM test and the ER-20-5 observation wells (Figure 1). The cavity radius (100 m), chimney height (1090 m), and melt-glass volume (3.22×10^5 m^3) are related empirically to the test yield (Pawloski, 1999). The domain is divided into a moderately sized grid with $95 \times 50 \times 65$ nodes, with grid spacing ranging from 7 m near the melt glass to 20 m away from the source. Model parameters, considered as effective properties, used in the simulations are listed in Table 1. Zero flow boundary conditions are imposed along the four sides parallel to the ambient flow direction. Pressure boundary conditions are imposed at the up and down gradient boundaries taking into account the hydrostatic increase in pressure with depth with a geothermal gradient of 0.01°C/m. The initial pressure and temperature distribution is obtained by first running to a steady state without the chimney-cavity-melt-glass present. The initial temperature of the melt glass is set to 290°C, just below the boiling point of water at depth, mainly to avoid two-phase conditions which would greatly complicate the calculations. However, this is a reasonable starting point for this investigation because only after single-phase conditions are reached is flow away from, rather than towards, the chimney likely to occur. Investigation of the rewetting period is left for future work.

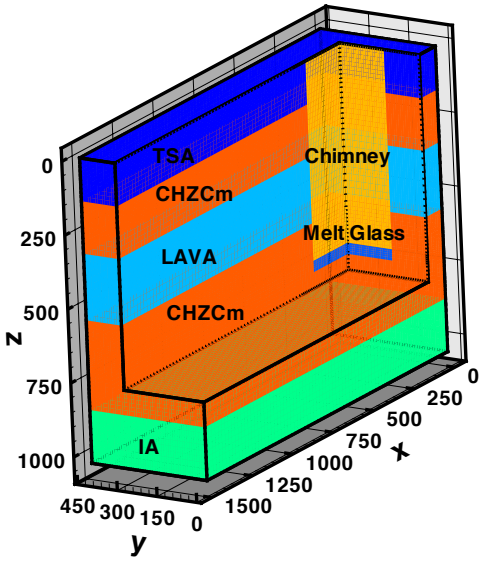

Figure 1: Cutaway view showing the grid used in the 3-D simulations. The position of the melt glass, chimney, and placement of TSA, upper CHZCm, LAVA, lower CHZCm, and IA stratigraphic units are indicated in the figure. Observation wells ER-20-5 #1 and #3, sampling in the TSA and LAVA aquifers, respectively, lie in the left y-z plane of the figure, 1.3 km from the chimney center.

Model simulations are carried out with the initial tracer concentration normalized to the initial concentration in the melt-glass pore volume and zero outside. Calibration is achieved by matching calculated breakthough curves to field data in wells ER-20-5 #1 and ER-20-5 #3. The lateral pressure gradient and effective LAVA porosity were used as fit parameters. A scale factor for each species is applied to the field data to obtain a match to the decay corrected breakthrough curves from wells ER-20-5 #1 and #3. The value of the scale factor provides an estimate of the corresponding initial radionuclide inventory for the mobile fraction of radionuclides measured in the observation wells. Four of the twelve radionuclide species detected in the ER-20-5 observation wells consisting of ^{3}H, ^{137}Cs, ^{239,240}Pu, and ^{36}Cl were modeled. These species represent short- and long-lived radionuclides, and those transported by colloids. A (possibly nonunique) match to the field data is achieved with a lateral flow gradient of 1 m/km and an effective LAVA porosity of 0.012. Although the four radionuclides considered to date represent the range in decay rates and transport properties of the entire set of radionuclides detected in the observation wells, complete analysis will require the consideration of all radionuclides detected.

Calculations are performed using the parallel computer code PFLOTRAN, a reactive flow and transport code developed at LANL. The code PFLOTRAN describes Darcy flow coupled to heat and multicomponent mass conservation equations. Although PFLOTRAN can account multicomponent chemical reactions including mineral precipitation and dissolution, sorption, and complexing reactions, in this study a single non-reactive tracer species is considered. PFLOTRAN is based on the PETSc parallel libraries developed at

Table 1: Stratigraphy and associated physical properties for different stratigraphic units representing the host rock at the BENHAM underground nuclear test (Wolfsberg et al., 2002), with the exception of the LAVA effective porosity which is treated as a fit parameter.

Unit Name	Depth [m]	ρ_r [kg/m^3]	c_r [J/(kg K)]	κ [J/(m s K)]	ϕ —	k [m^2]
TSA	0–145	2500	880	1.8	0.005	5.00×10^{-11}
CHZCm	145–320	2350	1154	1.2	0.250	2.00×10^{-14}
LAVA	320–550	2270	1000	2.5	0.012	1.00×10^{-12}
CHZCm	550–850	2350	1154	1.2	0.250	2.00×10^{-14}
IA	850–1050	2270	1000	2.5	0.083	5.00×10^{-13}
Chimney	0–714	2354	1043	1.8	0.185	1.00×10^{-11}
Glass	679–714	2500	1154	2.7	0.010	1.00×10^{-14}

Argonne National Laboratory (Balay et al., 1997) and makes use of object-oriented features in FORTRAN 90. PETSc (latest version 2.2.0) has achieved a high level of maturity that allows rapid development of efficient parallel implementation for solving systems of non-linear partial differential equations. PFLOTRAN is essentially platform independent and can run on any machine that PETSc runs on. This includes laptop computers, workstations, and massively parallel high performance computing facilities. PFLOTRAN uses a domain decomposition approach based on the fully implicit, non-linear, iterative solver (SNES) libraries in PETSc and uses the distributed array (DA) parallel data structure to manage communication between processors. This includes the local data owned by each processor and bordering grid cells owned by neighboring processors.

The simulations involve three degrees of freedom—pressure, temperature, and solute concentration—per grid block, resulting in a total of 308,750 $\times$ 3 = 926,250 degrees of freedom. Some savings in computation time could be obtained by solving the tracer transport equation sequentially from temperature and pressure since the latter equations do not involve the solute concentration, however, this savings is minimal when employing parallel computation with many processors. The calculations reported here were carried out on LANL's QSC and PNNL's MPP2 machines using 64 and 128 processors. Computation times scaled almost ideally with the number of processors. The memory requirements for this moderately sized problem are minimal compared to the available memory. On MPP2 each processor has 3-4 GB of memory, compared to 4 GB per processor on QSC. The advantages of parallel computing become even more pronounced as the complexity of the problem is increased, for example, by taking into account multicomponent processes and finer grid resolution. This would allow coupling competitive reactive processes for solute sorption to matrix materials and colloids as well as colloid filtration processes as described by Wolfsberg et al. (2002) into a three-dimensional simulation framework. For example, reducing the grid spacing by a factor of two in each direction would increase the number of degrees of freedom by eight. Increasing the number of chemical components to ten results in a four-fold increase in the degrees of freedom. Finally, including dual continuum capabilities with, for example, ten matrix nodes for each fracture node leads to an overall increase of $8 \times 4 \times 10 = 320$, or approximately 300 million degrees of freedom, which is beginning to stretch the limits of available computing facilities.

2.3 Results

Shown in Figure 2 is the calculated temperature distribution in the neighborhood of the test after an elapsed time of 10 years. Thermal plumes can be seen rising from the melt glass as it cools. As can be seen in the figure, buoyancy driven flow has reached the upper TSA aquifer and has carried the thermal plume along with radionuclides laterally. The melt glass temperature becomes highly nonuniform due to convective cooling. Apparent from this figure is that early breakthrough occurs in the upper TSA aquifer, and not the

LAVA where almost no temperature increase is visible after 10 years even though the LAVA unit is much closer to the source (see Figure 1). This is a consequence of the lower permeability and higher porosity of the LAVA compared to the TSA.

Radionuclide breakthrough curves for the 3-D simulation are shown in Figure 3 for ^{3}H, ^{137}Cs, ^{36}Cl, and ^{239,240}Pu. A good match to field observations in wells ER-20-5 #1 and #3, indicated by the symbols, is obtained for ^{3}H, ^{137}Cs, and ^{36}Cl, by fitting to the tracer breakthrough curve corrected for radioactive decay. Radioactive decay is included for ^{3}H and ^{137}Cs by transforming the breakthrough concentrations by the decay factor $\mathrm{e}^{-\lambda t}$, with λ corresponding to tritium and cesium half lives of 12.32 y and 30.2 y, respectively (radioactive decay of ^{36}Cl and ^{239,240}Pu with half lives of 301,000 years and 24,100/6560 years, respectively, is negligible over the time scale of these simulations). In particular, the coupled model is able to explain the relative magnitude in concentrations observed in the upper TSA and lower LAVA aquifers. The results of the calculations are consistent with the interpretation that species ^{3}H and ^{36}Cl move unretarded, as well as some portion of ^{137}Cs and ^{239,240}Pu sorbed irreversibly to colloids. However, they do not require that there be no retardation. For example, if a smaller value is used for the chimney porosity, then retardation (or refitting the lateral flow gradient) would be necessary to obtain the observed breakthrough times. For a flow dominated system, the porosity times the retardation factor appears in the transport equation and the two quantities cannot be determined separately [see Eqn.(1c)]. Note that this analysis does not provide an estimate of what fraction of the reactive species sorb to colloids, or what fraction of colloids filter out of the flow system.

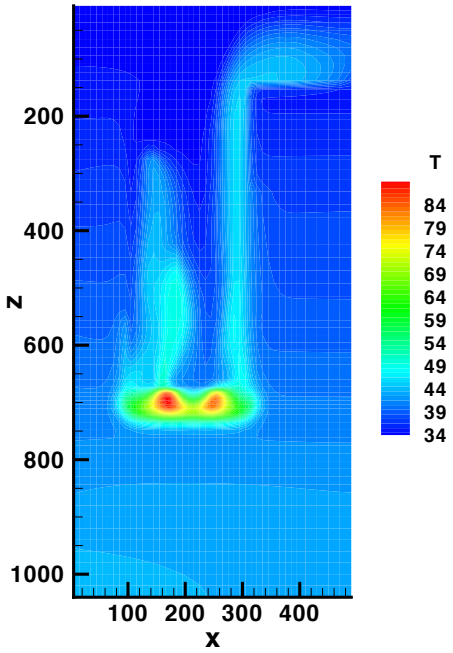

Figure 2: Near-field temperature distribution after an elapsed time of 10 years.

Transport of the species ^{239,240}Pu appears to be an anomaly. Comparison of the measured ^{239,240}Pu concentrations with the tracer breakthrough curves would suggest that ^{239,240}Pu is moving more rapidly than a tracer (due to the smaller ratio between the measured concentrations in the TSA and LAVA). To obtain a match between model results and field data with a single scale factor for ^{239,240}Pu, a colloid velocity enhancement factor or smaller effective porosity is required. Shown in the figure is a fit to the ^{239,240}Pu breakthrough curve with an enhancement factor of $f_c = 1.06$ (compared to a maximum theoretical value of $f_c = 1.5$). This is equivalent to using an effective LAVA porosity of 0.012/1.06 = 0.0113, and chimney porosity of 0.185/1.06 = 0.175. Although these changes in porosity seem relatively minor, they can have a large effect on the travel time because of the small value of the porosity. Thus for a change $\Delta\phi$ in porosity, the travel time $\tau(\phi)$ becomes $\tau(\phi) \simeq \tau(\phi_0)(1 + \Delta\phi/\phi_0) = \tau(\phi_0)/f_c$.

It is reasonable to assume that the effective porosity used in the simulations, calibrated to the ^{3}H simulation, does not apply to colloids to explain the ^{239,240}Pu anomaly. In fact, the effective porosity experienced by a colloid should be less, because colloids generally do not participate in matrix diffusion as can conservative solutes. However, this does not explain why ^{137}Cs, also apparently transported irreversibly on colloids, does not exibit the more rapid migration experienced by ^{239,240}Pu. One possible explanation is that they are associated with different colloids with very different transport and radionuclide sorption properties. The species ^{137}Cs is a strongly sorbing cation which undergoes ion exchange and does not readily form complexes, whereas ^{239,240}Pu sorbs through surface complexation reactions and forms strong complexes with carbonate. Column transport experiments have been performed showing that ^{239,240}Pu sorbs nearly irreversibly zeolite colloids while sorbing reversibly on silica and clay colloids (Kersting and Reimus, 2003). Similar experiments for ^{137}Cs might elucidate the reversibility of that species on colloids and provide

insight regarding the slightly different apparent velocities for ^{239,240}Pu and ^{137}Cs.

The scale factors in units of pCi/L obtained for each species by matching the breakthrough curve in the TSA to wells ER-20-5 #1 and #3 are listed in Table 2. The scale factors provide an estimate of the initial radionuclide inventory in Curies by multiplying by the melt-glass volume of 3.22×10^5 m^3 and porosity of 1%, to give the values listed in Table 2. It should be noted, however, that for the case of strongly sorbed species such as is expected for ^{137}Cs and ^{239,240}Pu, only the mobile species fraction that is irreversibly sorbed on colloids is accounted for in this estimate.

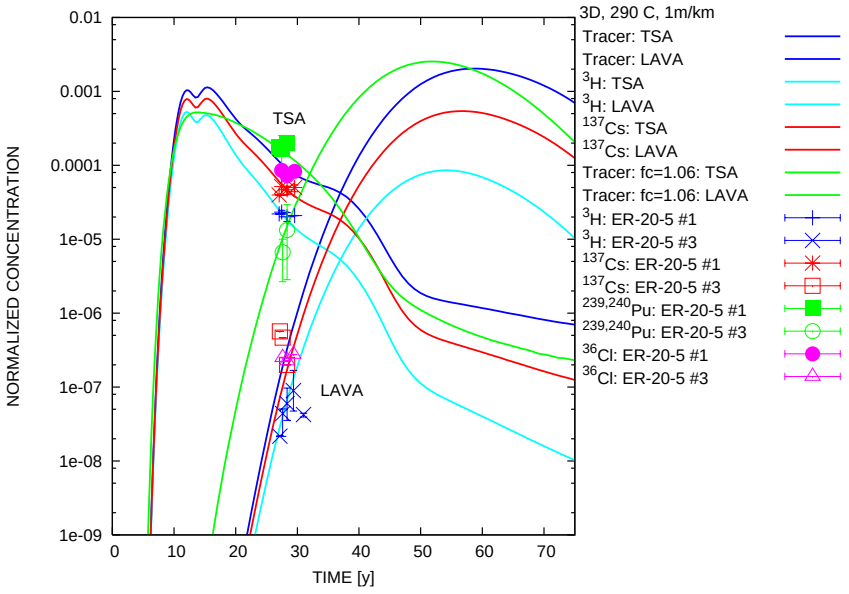

Figure 3: Breakthrough curves in the TSA and LAVA stratigraphic units for a 3-D simulation of a non-reactive tracer released from the melt glass. The breakthrough curves are corrected for radioactive decay of tritium and cesium (12.32 y and 30.2 y half lives). The measured ^{239,240}Pu breakthrough concentrations were fit with $f_c = 1.06$. Symbols represent field measurements from wells ER-20-5 #1 and #3 (Wolfsberg et al., 2002; Finnegan and Thompson, 2003), for the indicated radionuclide scaled by the factors listed in Table 2.

The simulation predicts a pulse release of radionuclides to the TSA and LAVA aquifers. Peak releases occur at roughly 15 y for the TSA unit and 55 y for the LAVA unit. This behavior is caused by the localized source terms for solute and heat in the initial melt glass configuration. Release of heat from the melt glass and formation of convection cells which drive fluid up the chimney, and its subsequent cooling and collapse of convective transport is, however, primarily responsible for the pulse behavior. Multicomponent, two-dimensional simulations of this system which include a kinetic model for dissolution of the melt glass and release of radionuclides also exhibit a pulse release through the temperature dependence of the dissolution rate which dramatically slows as the melt glass cools (Wolfsberg et al., 2002). The 3-D simulations suggest that tritium in well ER-20-5 #3 is just beginning to increase. However, the last ^{3}H observation point suggests that the peak in tritium has already occurred, marked by the observed drop in the tritium concentration in well ER-20-5 #3. This last data point was reported by Finnegan and Thompson (2003) for well ER-20-5 #3 (a pump failure occurred in well #1) taken on November, 2001. They measured ^{237}Np, ^{85}Kr and ^{3}H, and found no detectable ^{137}Cs. It should be noted, however, that the measurements from ER-20-5 #3 are close to the detection limit. Further data will be needed to confirm whether the model is correct and tritium and the other radionuclide concentrations are still increasing with time in well ER-20-5 #3.

There are a number of simplifying assumptions and uncertainties that may affect the results in this study. Fluxes through the aquifers are sensitive to the specified effective permeabilities. Single well tests indicate variations in permeability of several orders of magnitude within individual hydrostratigraphic units (Rehfeldt et al., 2004). Increasing the flux by increasing the head gradient to 2 m/km led to reversed order in concentrations with the larger value in the LAVA compared to the TSA and it was not possible to obtain a match to the field data. Additionally, fracture-matrix interactions (matrix diffusion in this case) are not accounted for explicitly. Extension to a dual continuum model formulation would enable incorporation of matrix diffusion, but this feature has not yet been incorporated into PFLOTRAN. The calculations do suggest, however, that the equivalent continuum representation of effective porosity is not valid. In this

limiting case, the effective porosity is given by $\phi = \epsilon_f \phi_f + (1-\epsilon_f)\phi_m \simeq \phi_m$, for $\epsilon_f \ll 1$. Considering that fracture porosities are very small and that the TSA and LAVA matrix porosities have the values 0.16 and 0.08 (Wolfsberg et al., 2002), respectively, this would give much larger values for the effective porosities than used in the simulation. Breakthrough times at ER-20-5 #1 in the TSA aquifer are rather insensitive to the TSA effective porosity provided it is sufficiently small because the travel time is dominated by flow through the chimney, but breakthrough at ER-20-5 #3 in the LAVA is very sensitive to the effective LAVA porosity, which is used as a fit parameter. However, these results suggest that in the TSA aquifer, because of its small effective porosity and fast travel time, matrix diffusion affects on non-reactive solutes and radionuclides irreversibly sorbed to colloids should be small. Finally, it should be noted that the initial distribution of radionuclides depends on the individual species (Pawloski et al., 2001). Radionuclides may be contained primarily in the melt glass (e.g. ^{239,240}Pu), or distributed throughout a much larger volume including the cavity and chimney but excluding the melt glass (e.g. ^{3}H), or be divided equally between the melt glass and cavity-chimney (e.g. ^{36}Cl). The particular distribution of each species would clearly affect the travel time to the TSA through the chimney.

Table 2: Scale factors used to fit measured radionuclide concentrations in well ER-20-5 #1 and #3 for a unit source concentration and the estimated mobile fraction of the initial inventory.

Radionuclide	Scale Factor [pCi/L]	Estimated Inventory [Ci]
^{3}H	3×10^{12}	9.66×10^{6}
^{36}Cl	4×10^{4}	0.129
^{137}Cs*	1×10^{6}	3.22
^{239,240}Pu*	3×10^{3}	0.01

* Mobile fraction irreversibly sorbed on colloids.

3 CONCLUSION

Three-dimensional simulations at the field scale demonstrate the feasibility of matching field data documenting radionuclide migration from the BENHAM underground nuclear test and thereby narrowing the range of uncertainty in model simulations. The model simulations show a pulse release of radionuclides to the TSA aquifer over a narrow window in time through the creation of convection cells caused by heat released from the melt glass. Field data from wells ER-20-5 #1 and #3 for radionuclides ^{3}H, ^{36}Cl, and ^{137}Cs could be explained assuming a non-reactive tracer with concentrations adjusted for radioactive decay, although additional data is needed to confirm the trend in time. Through the use of effective properties for porosity and permeability, allowance could be made for matrix diffusion processes, the extent of which may be limited by high flow velocities and possibly fracture coatings that inhibit matrix diffusion. The radionuclide ^{239,240}Pu presented an anomaly in the fit to the field data, which indicated it was moving faster than the other three radionucldes considered. While this is consistent with the hypothesis that ^{239,240}Pu transport is colloid-facilitated, because the fit to the ^{137}Cs field data also indicated colloid-facillitated transport but at somewhat slower migration rates than ^{239,240}Pu, presumably different types of colloids were involved for ^{239,240}Pu and ^{137}Cs. The results presented here appear to be the first indication that field scale colloid transport can involve flow velocities faster than a non-reactive tracer species.

Because simulations of radionuclide migration from an underground nuclear test, such as the BENHAM test, are intrinsically 3-D as a result of the unique cavity-chimney-melt-glass geometry, massively parallel high performance computing is required to tackle these problems. Using the computer code PFLOTRAN it is now possible to carry out such calculations on available computing facilities such as LANL's QSC nonclassified alpha cluster, as well as other machines including EMSL's MPP2 Intel Itanium-2 cluster at PNNL. However, it should perhaps be emphasized that high performance computing can help alleviate, but not eliminate, upscaling and multiscale issues. However, high performance computing will make more feasible multiple continuum models which can incorporate length scales ranging from perhaps millimeters to meters for describing multicomponent-multiphase systems in fractured porous media.

Future work will consider the relatively immobile radionuclide fraction through the addition of multicomponent chemical reactions including reversible and irreversible sorption, complexation, and precipi-

tation and dissolution reactions to describe alteration of the melt glass, and implementation of a dual continuum description of fracture-matrix interaction. The effect of grid refinement on convection cells formed during the cooling period will be investigated. Finally, the rewetting phase of the near-field region and its effect on radionuclide release times will be considered.

4 ACKNOWLEDGEMENTS

We would like to thank Robert M. Bangerter, NNSA Underground Test Area (UGTA) manager, for supporting our initial studies (Wolfsberg et al., 2002), and for review and advice regarding this manuscript. Hari Viswanathan provided a helpful review of an earlier version of the manuscript. We also thank Richard Mills and Glenn Hammond for help with implementing parallel computing using PETSc. This research was performed in part using the MSCF in EMSL, a national scientific user facility sponsored by the U.S. DOE, OBER and located at PNNL, and the QSC machine at LANL. This work was funded in part by the Los Alamos National Laboratory LDRD-DR project 20030091DR.

5 REFERENCES

Balay, S., W.D. Gropp, L.C. McInnes and B.F. Smith. 1997. Efficient Management of Parallelism in Object Oriented Numerical Software Libraries, Modern Software Tools in Scientific Computing, E.Arge, A.M. Bruaset and H.P. Langtangen, Ed., Birkhauser Press, Boston, MA, 163-202.

Department of Energy. 2000. United States Nuclear Tests-July 1945 through September 1992. US Department of Energy, Nevada Operations Office, Las Vegas, NV, DOE/NV-209 (Rev. 15).

Honeyman, B. D., and J. F. Ranville. 2002. Colloid properties and their effects on radionuclide transport through soils and groundwater, in Geochemistry of Soil Radionuclides, edited by P.-C. Zhang, and P.V. Brady, pp. 131–163, Soil Science Society of America, Special Publication Nr. 59, Madison, WI.

Finnegan, D.L. and J.L. Thompson. 2003. Laboratory and Field Studies Related to Radionuclide Migration at the Nevada Test Site in Support of the Underground Test Area Project and Hydrologic Resources Management Project, October 1, 2001 - September 30, 2002, Los Alamos National Laboratory LA-14042-PR, Los Alamos, NM.

Kersting, A.B., D.W. Efurd, D.L. Finnegan, D.J. Rokop, D.K. Smith, and J.L. Thompson. 1999. Migration of plutonium in groundwater at the Nevada Test Site, Nature 397: 56–59.

Kersting, A.B., and P.W. Reimus. 2003. Colloid-Facilitated Transport of Low-Solubility Radionuclides: A Field, Experimental, and Modeling Investigation, UCRL-ID-149688. Lawrence Livermore National Laboratory, Livermore, CA; and Los Alamos National Laboratory, Los Alamos, NM.

Lichtner, P.C. 2000. Critique of Dual Continuum Formulations of Multicomponent Reactive Transport in Fractured Porous Media, *Dynamics of Fluids in Fractured Rock*, Geophysical Monograph **122**, 281–298.

Pawloski, G.A. 1999. Development of phenomenological models of underground nuclear tests on Pahute Mesa, Nevada Test SiteBENHAM and TYBO, Lawrence Livermore National Laboratory, UCRL-ID-136003.

Pawloski, G.A., A.F.B. Tompson, and S.F. Carle (eds.). 2001. Evaluation of the hydrologic source term from underground nuclear tests on Pahute Mesa at the Nevada Test Site: The Cheshire test, Lawrence Livermore National Laboratory, UCRL-ID-147023.

Rehfeldt, K., W. Drici, B. Lester, D. Sloop, J. Watrus, T.Beard, M. Sully, W. Fryer, and C. Benedict. 2004. Hydrologic Data for the Groundwater Flow and Contaminant Transport Model of Corrective Action Units 101 and 102: Central and Western Pahute Mesa, Nye County, Nevada. Technical report S-N/99205–002, Stoller-Navaro, Las Vegas Nevada.

Wolfsberg, A., L. Glascoe, G. Lu, A. Olson, P. Lichtner, M. McGraw, T. Cherry, and G. Roemer. 2002. TYBO/BENHAM: Model Analysis of Groundwater Flow and Radionuclide Migration from Underground Nuclear Tests in Southwestern Pahute Mesa, Nevada, Los Alamos National Laboratory LA-13977, Los Alamos, NM.